Iron reduction in profundal sediments of ultra-oligotrophic Lake Tahoe under oxygen-limited conditions

Supporting Information

Meret Aeppli[1,2,*], Geoffrey Schladow[3,4], Juan S. Lezama Pacheco[1,5], and Scott Fendorf[1]

[1]*Department of Earth System Science, Stanford University, Stanford, California* 94305*, United States*
[2]*School of Architecture, Civil and Environmental Engineering, EPFL,* 1015 *Lausanne, Switzerland*
[3]*Department of Civil and Environmental Engineering, UC Davis, Davis, California* 95616*, United States*
[4]*UC Davis Tahoe Environmental Research Center, Incline Village, Nevada* 89451*, United States*
[5]*Stanford Synchrotron Radiation Lightsource, SLAC National Accelerator Laboratory, Menlo Park, California* 94025*, United States*

* correspondence: meret.aeppli@epfl.ch

12 Pages, 11 Figures, 2 Tables

List of Figures

List of Tables

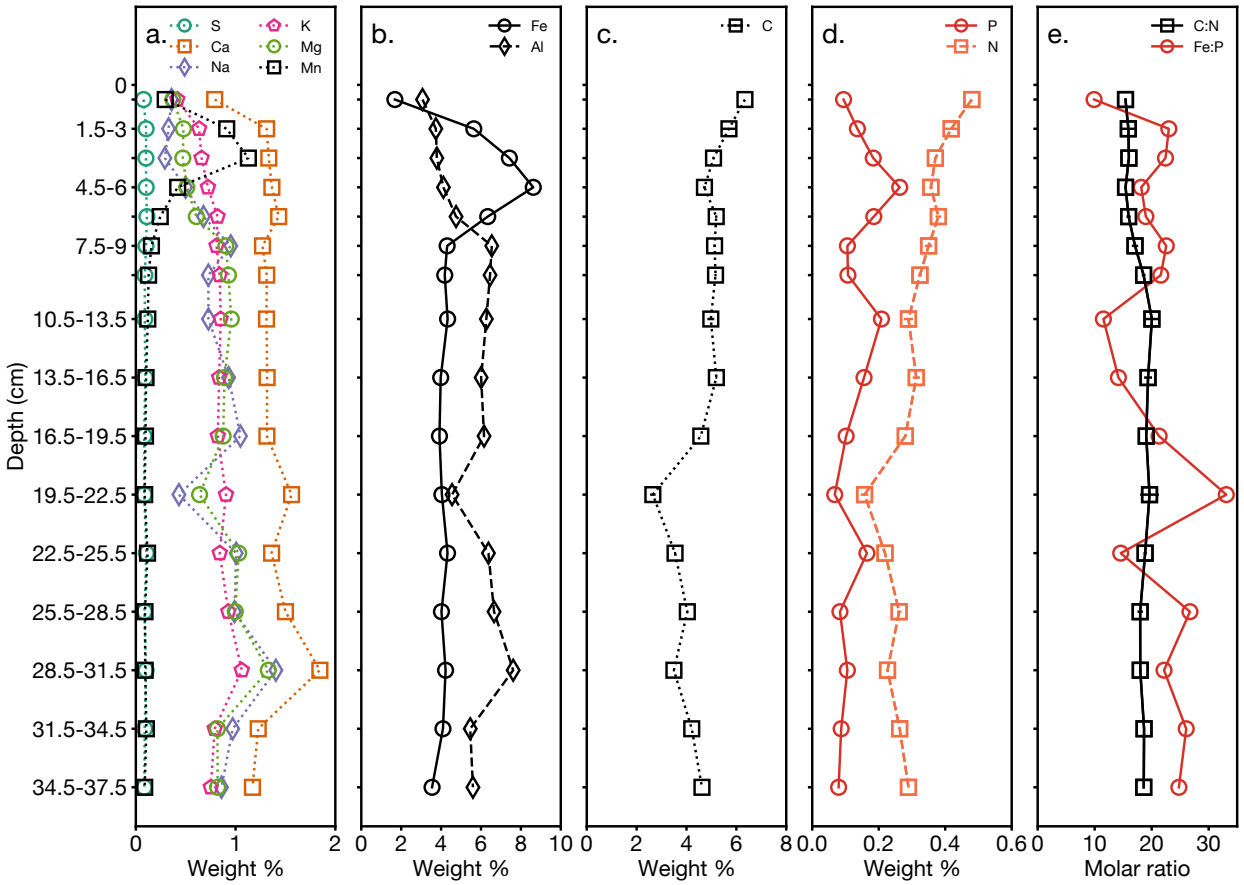

Figure S1. Sediment elemental composition. Concentrations of total **a.** sulfur (S), calcium (Ca), sodium (Na), potassium (K), magnesium (Mg), manganese (Mn), **b.** iron (Fe), aluminum (Al), **c.** carbon (C), **d.** phosphorus (P), and nitrogen (N). **e.** Molar ratios of C:N and Fe:P. Error bars for C and N represent mean absolute deviations of duplicate measurements on single samples. Analyses were performed on sediment cores that were frozen after collection to represent in-situ conditions in the lake.

Table S1. Sediment density in cores used for incubation experiments under 0.1 %, 5.5 %, and 21 % atmospheric oxygen. Values represent averages and standard deviations of eight samples collected at each depth from 0 to 74 d of the experiment.

Treatment	Depth (cm)	Sediment density av (g/cm^3)	Sediment density dev (g/cm^3)
0.1%	0.5	0.175	0.063
	1.5	0.206	0.042
	3	0.204	0.039
	4.5	0.200	0.064
	6	0.275	0.056
	7.5	0.290	0.027
5.5%	0.5	0.166	0.037
	1.5	0.179	0.026
	3	0.213	0.043
	4.5	0.233	0.043
	6	0.261	0.042
	7.5	0.250	0.049
21%	0.5	0.179	0.040
	1.5	0.223	0.068
	3	0.217	0.045
	4.5	0.245	0.058
	6	0.289	0.051
	7.5	0.247	0.047

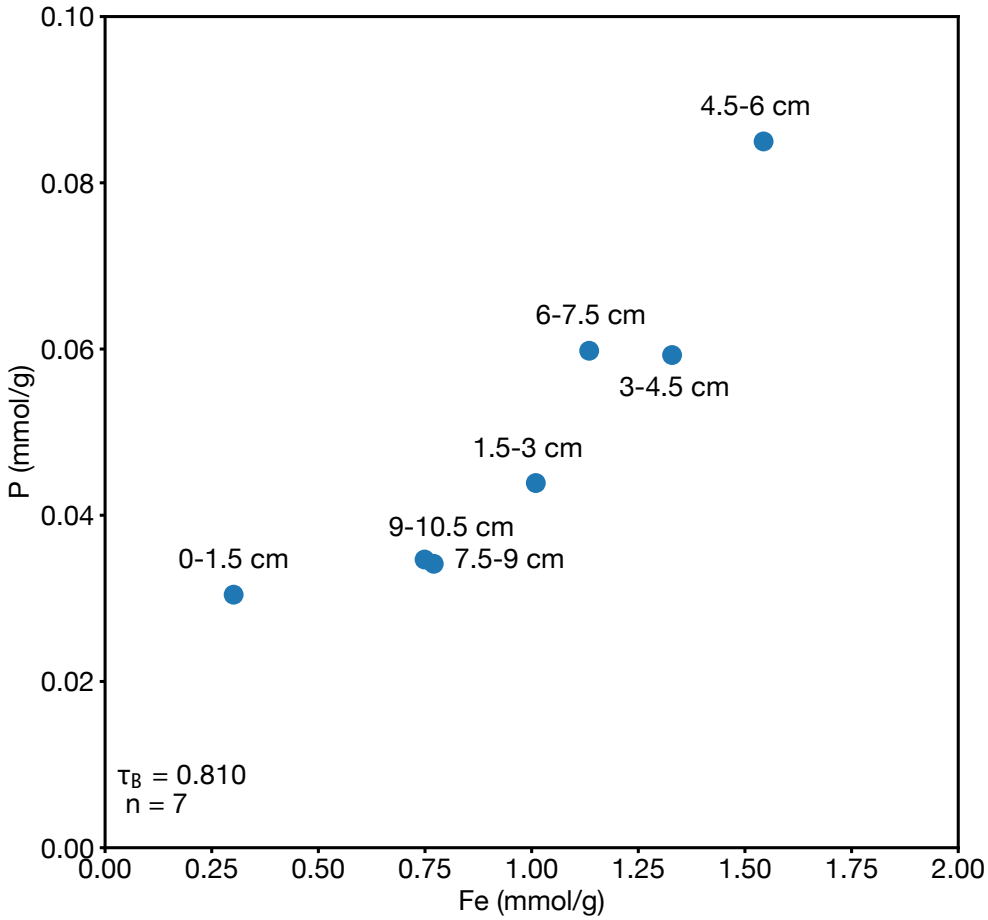

Figure S2. Relationship between Fe and P sediment contents for 0 to 10.5 cm depth. Concentrations of total P are plotted versus concentrations of total Fe. Kendall rank correlation analysis was performed on the data using the kendalltau function in the scipy stats module in Python. The number of data points included in the analysis (n) and Kendall's τ_B values (τ_B = 1: perfect positive correlation and τ_B = 0: no correlation) are reported. Analyses were performed on sediment cores that were frozen after collection to represent in-situ conditions in the lake.

Table S2. Relative proportions of Fe species as determined on Fe K-edge EXAFS spectra using linear combination-least squares fitting. Analyses were performed on sediment cores that were frozen after collection to represent in-situ conditions in the lake. Phases used in the fit were ferrihydrite[1] (Fe oxyhydroxide); ferrosmectite, nontronite[2] (phyllosilicate minerals: 2:1 clays), biotite[3] (phyllosilicate minerals: mica); and hornblende (inosilicate minerals). Fits are shown in Figure S3.

Depth (cm)	Ferri-hydrite (%)	Ferro-smectite (%)	Nontronite (%)	Biotite (%)	Hornblende (%)	R-factor (%)	Reduced χ^2
1.5-3 cm	35	53		11		0.021	0.117
3-4.5 cm	32	56		12		0.024	0.138
4.5-6 cm	39	52		10		0.022	0.122
6-7.5 cm	44	46		10		0.022	0.114
31.5-34.5 cm	16	21	18	22	24	0.014	0.087

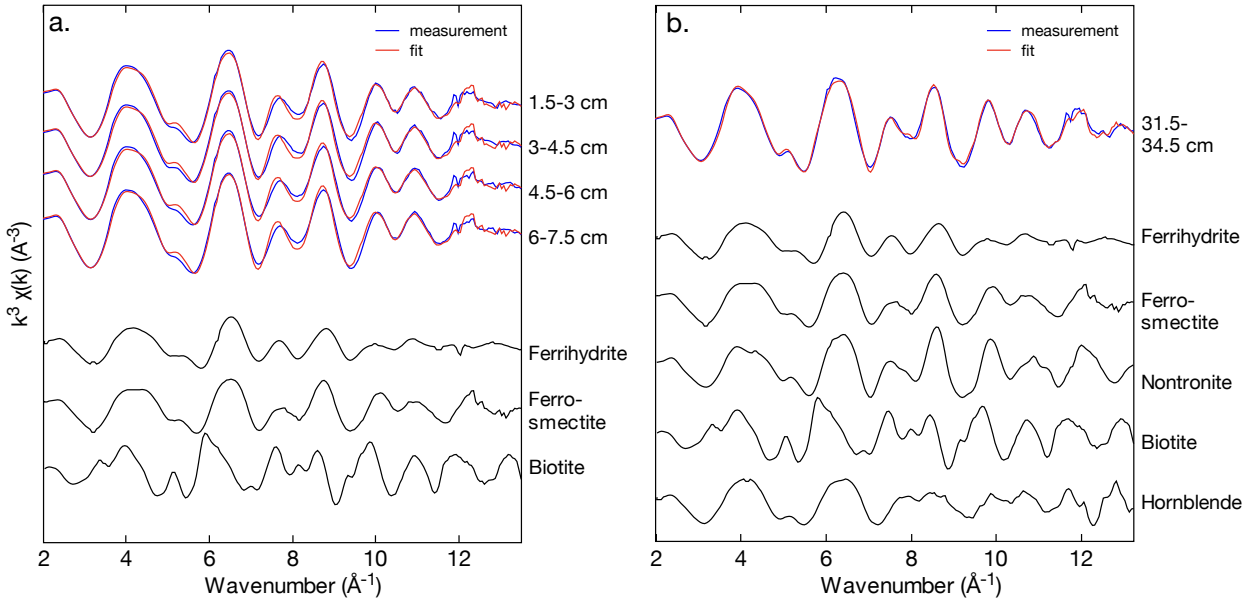

Figure S3. Fourier transforms of bulk Fe K-edge EXAFS spectra (blue lines) and linear combination-least squares fit (red lines) for sediment samples collected at **a.** 1.5-7.5 cm and **b.** 31.5-34.5 cm depth. References are shown in black and include ferrihydrite[1] (Fe oxyhydroxide); ferrosmectite, nontronite[2], biotite (phyllosilicate minerals)[3]; and hornblende (inosilicate mineral). Fitted relative proportions of Fe species are shown in Table S2.

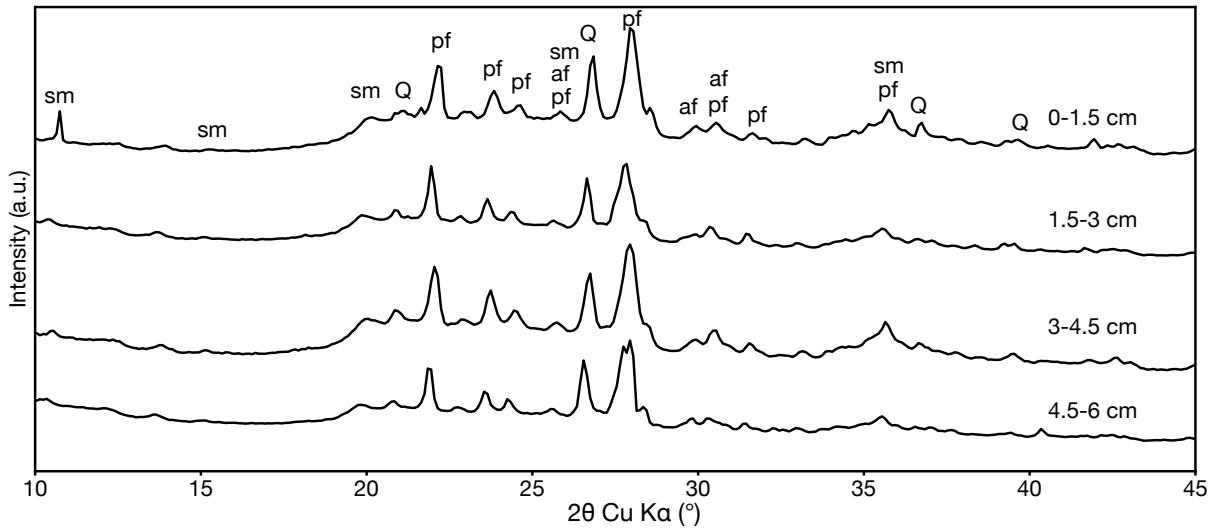

Figure S4. Representative X-ray diffractograms for sediment samples collected at 1.5-7.5 cm depth. Characteristic peaks for quartz (Q), and members of the plagioclase feldspar (pf), alkali feldspar (af) and smectite (sm) groups are labelled on the plot.

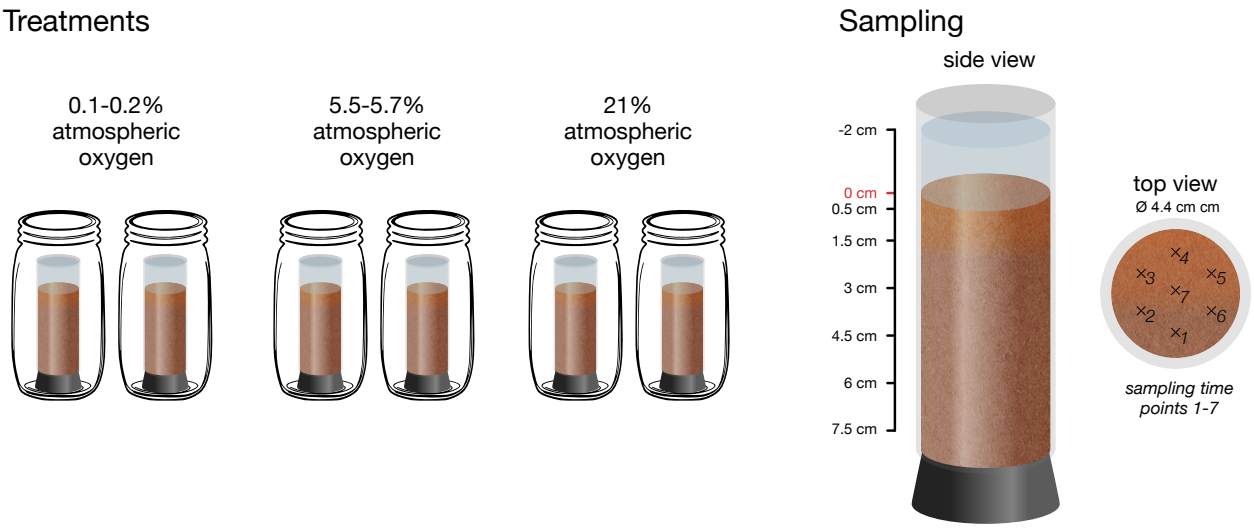

Figure S5. Setup of whole-core incubation experiments. Whole cores were incubated in sealed jars at three atmospheric oxygen levels of 0.1 - 0.2 %, 5.5 - 5.7 %, and 21 % and at 5° C (duplicate cores for each treatment). Sediment aliquots were sampled from 0.5 cm, 1.5 cm, 3 cm, 4.5 cm, 6 cm and 7.5 cm depth at each sampling point as indicated in the illustration.

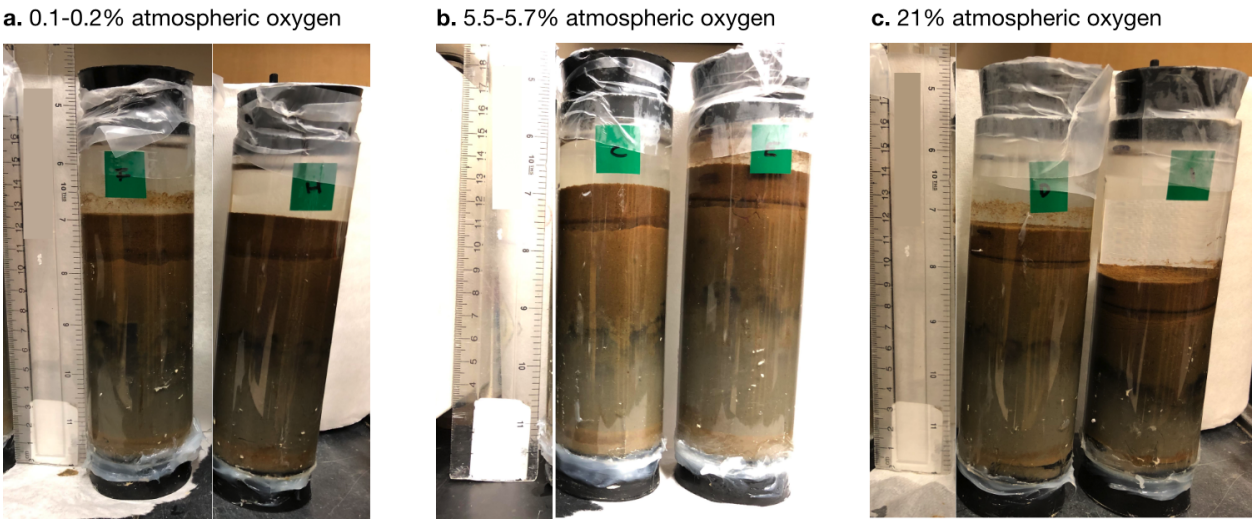

Figure S6. Photos of cores used in incubation experiments at **a.** 0.1 - 0.2 % atmospheric oxygen, **b.** 5.5 - 5.7 % atmospheric oxygen, and **c.** 21 % atmospheric oxygen. The top layer of slightly darker sediment material was less consolidated than layers below and moved with overlaying water.

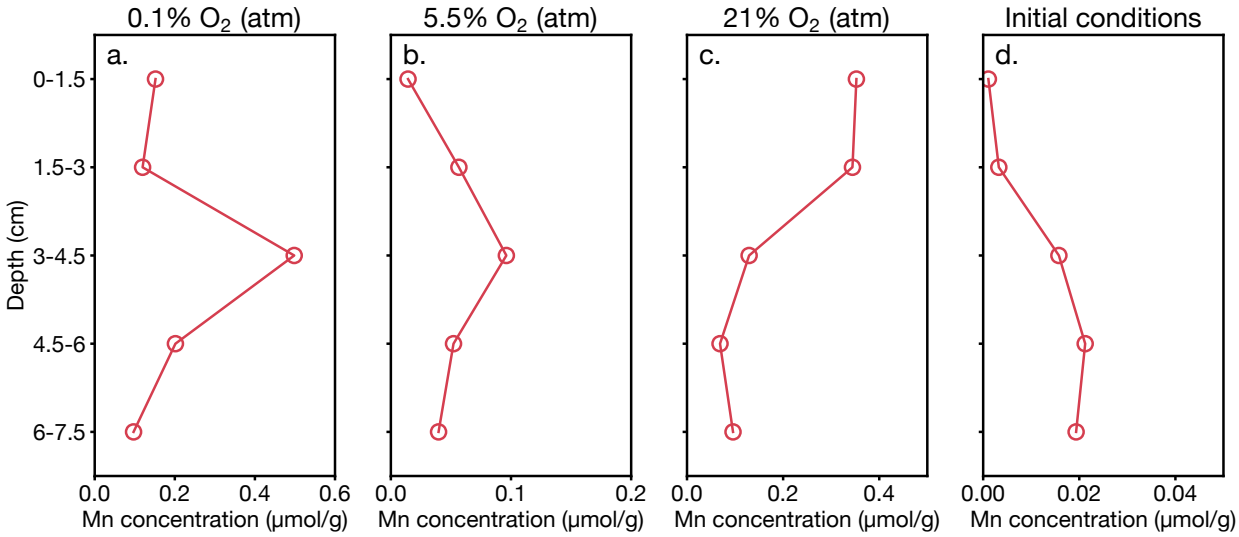

Figure S7. Profiles of water-extractable Mn. **a.-c.** Profiles measured at the endpoint of whole-core incubation experiments at 0.1 %, 5.5 %, and 21 % atmospheric oxygen. **d.** Profile measured on a core that was frozen after collection to represent in-situ conditions in the lake and initial conditions for the incubation experiments. Water extractions were performed as described in the Materials and Methods section.

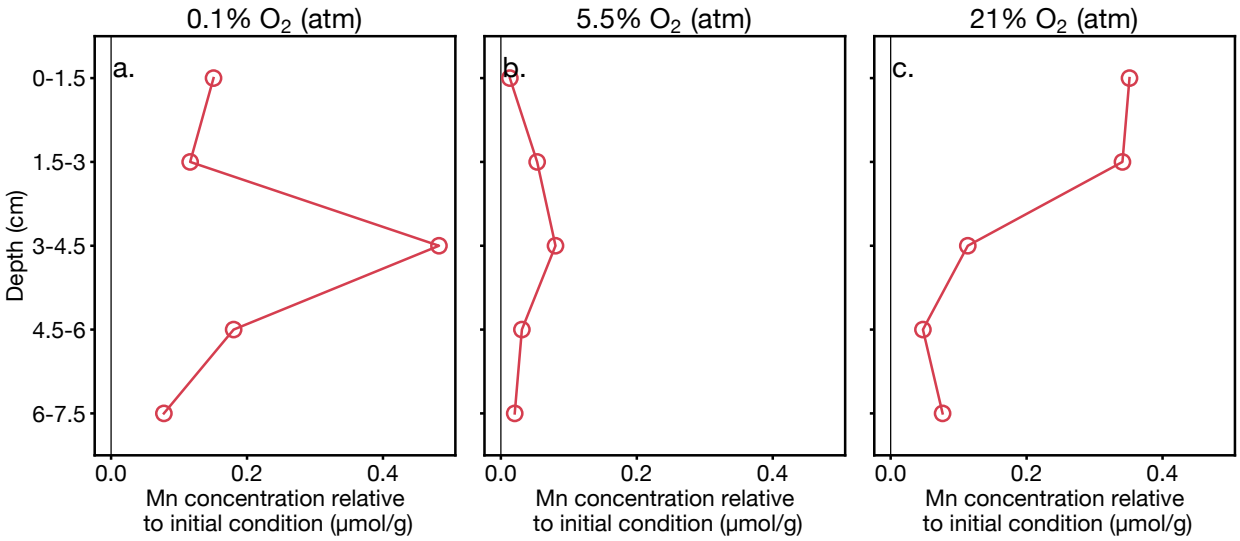

Figure S8. Change in water-extractable Mn in whole-core incubation experiments at **a.** 0.1 %, **b.** 5.5 %, and **c.** 21 % atmospheric oxygen. Changes in concentrations were calculated as the difference in endpoint concentrations (Figure S7a-c) relative to initial conditions (Figure S7d).

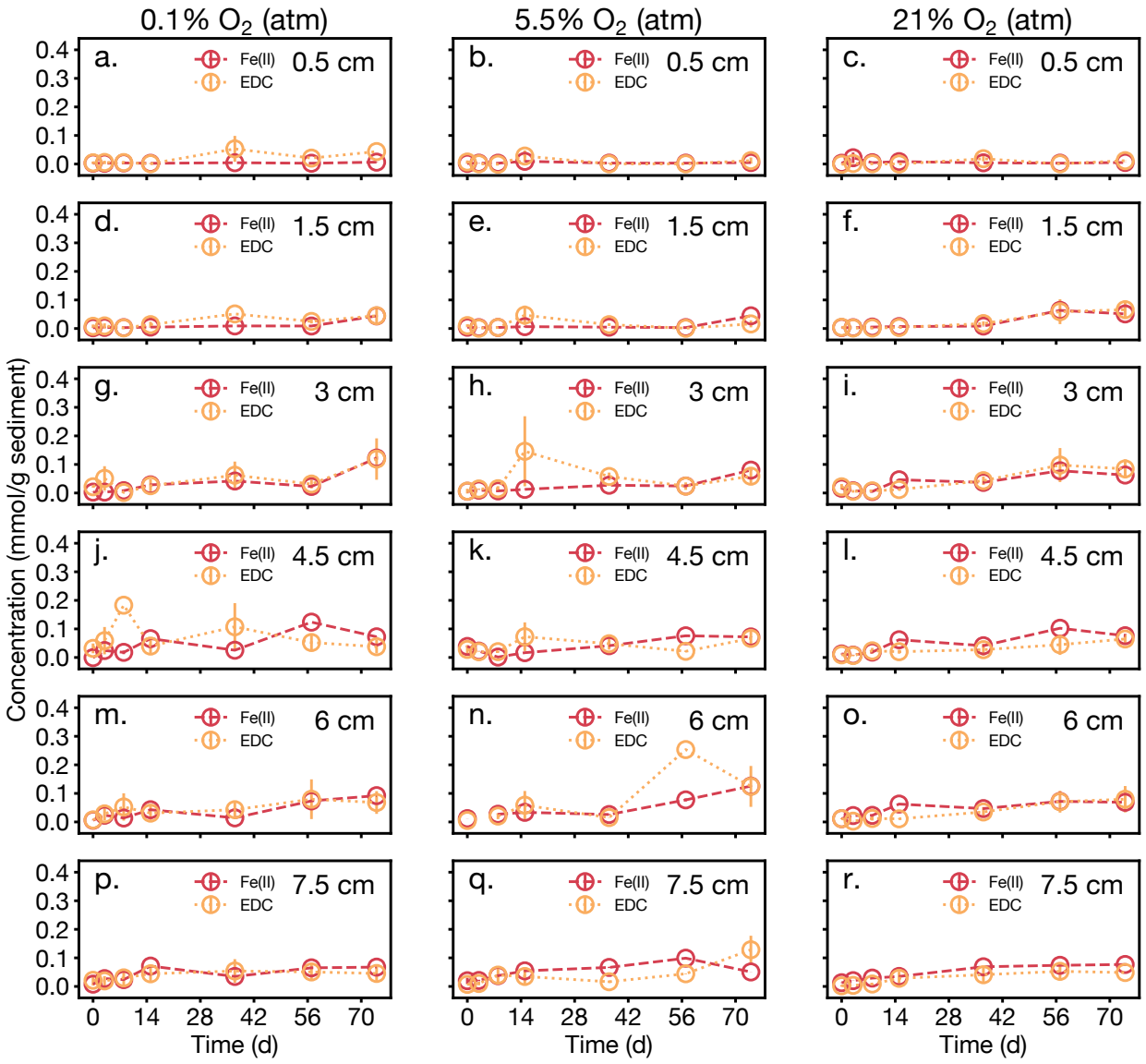

Figure S9. Increase in electron donating capacity (EDC) and 0.5 HCl-extractable Fe(II) over the course of whole-core incubation experiments at 0.1 % (left column), 5.5 % (middle column), and 21 % atmospheric oxygen (right column). Error bars represent mean absolute deviations of duplicate measurements on pooled sediment samples from the duplicate cores.

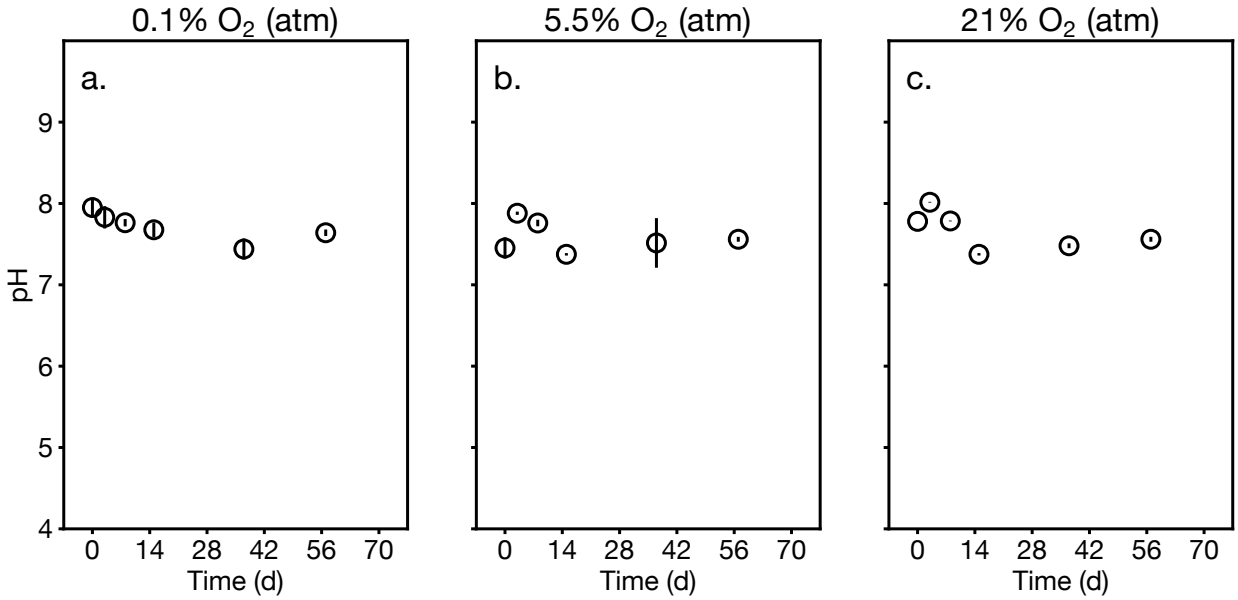

Figure S10. Variations in pH of water overlaying sediments in whole-core incubation experiments at **a.** 0.1 %, **b.** 5.5 %, and **c.** 21 % atmospheric oxygen. Error bars represent mean absolute deviations of measurements performed on duplicate cores.

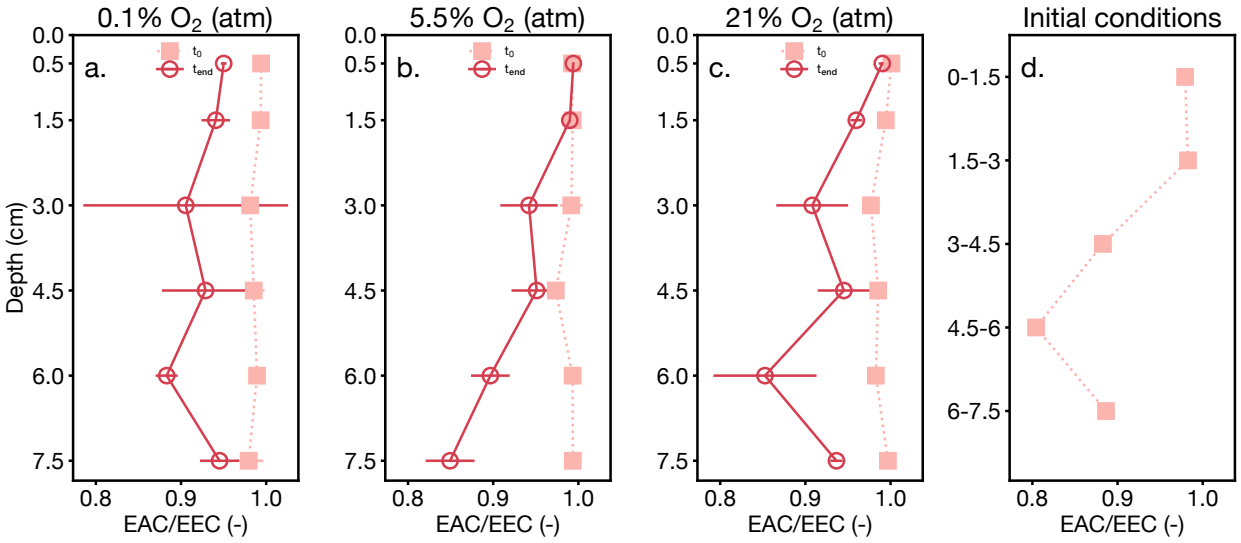

Figure S11. Profiles of electron accepting capacity (EAC) over electron exchanging capacity (EEC, sum of EAC and electron donating capacity) at the start (t_0) and end (t_{end}) of whole-core incubation experiments at **a.** 0.1 %, **b.** 5.5 %, and **c.** 21 % atmospheric oxygen. **d.** For comparison, EAC/EEC profile of a core that was frozen after collection to represent in-situ conditions in the lake and initial conditions of the incubation experiments. Error bars represent mean absolute deviations of duplicate measurements on pooled sediment samples from the duplicate cores.

References

1. Maillot, F. *et al.* New insight into the structure of nanocrystalline ferrihydrite: EXAFS evidence for tetrahedrally coordinated iron(III). *Geochim Cosmochim Acta* **75**, 2708–2720 (2011).

2. Noël, V. *et al.* EXAFS analysis of iron cycling in mangrove sediments downstream a lateritized ultramafic watershed (Vavouto Bay, New Caledonia). *Geochim Cosmochim Acta* **136**, 211–228 (2014).

3. Othmane, G. *et al.* Uranium Association with Iron-Bearing Phases in Mill Tailings from Gunnar, Canada. *Environ Sci Technol* **47**, 12695–12702 (2013).